01 Jan 1971

Calculation Of Anisotropic Hyperfine Constants For Lattice Nuclei Near A Shallow Donor

Edward B. (Boyd) Hale
Missouri University of Science and Technology, ehale@mst.edu

Robert Lee Mieher

Recommended Citation

E. B. Hale and R. L. Mieher, "Calculation Of Anisotropic Hyperfine Constants For Lattice Nuclei Near A Shallow Donor," *Physical Review B*, vol. 3, no. 6, pp. 1955 - 1965, American Physical Society, Jan 1971.
The definitive version is available at https://doi.org/10.1103/PhysRevB.3.1955

Calculation of Anisotropic Hyperfine Constants for Lattice Nuclei near a Shallow Donor*

Edward B. Hale† and Robert Lee Mieher
Department of Physics, Purdue University, Lafayette, Indiana 47907
(Received 19 October 1970)

A method is presented for calculating the magnetic anisotropic (dipolar) hyperfine constants for lattice nuclei near a shallow-donor impurity. The method assumes that the wave function of the donor electron can be expressed in an effective-mass form, i.e., a slowly varying envelope function times conduction-band Bloch functions. For each dipolar hyperfine constant, two separate calculations are performed. One calculation is for a local region about the lattice nucleus of interest. The greatest part of the interaction occurs in this region (about 85 ±10%). The second calculation is for the more distant region. The dipolar constants in the distant region are calculated without considering the details of the Bloch functions and are evaluated by an integration involving only the envelope function. In the local region, the details of the Bloch functions must be considered. The Bloch functions are expressed in terms of equivalent orbitals. Symmetry arguments using the properties of these orbitals simplify the calculation. The final results show that the local contribution can be expressed as products of a few intrinsic lattice parameters, which are the dipolar matrix elements between equivalent orbitals, and a set of coefficients that is not difficult to evaluate. The resulting dipolar constants vary a great deal from one lattice site to another. Numerical results have been computed for the shallow donors – arsenic, phosphorus, and antimony – in silicon. Comparison of theoretical values with experimental values shows qualitative and semiquantitative agreement.

I. INTRODUCTION

Many properties of shallow impurity centers in semiconductors can be understood through the effective-mass model as formulated by Kohn and Luttinger.[1-3] An example is the calculation of the isotropic or Fermi contact hyperfine interaction between the unpaired impurity electron and a lattice nucleus, which has been discussed in detail by Feher[4] and, more recently, by Hale and Mieher.[5,6] Their essential conclusions were that these isotropic constants can be qualitatively understood in terms of the effective-mass theory, but that refinements are still necessary to obtain quantitative agreement with the experimental results. The anisotropic or dipolar hyperfine interactions have not even been qualitatively understood. Understanding the physical origin of these interactions in detail has become more important recently since new electron-nuclear double-resonance (ENDOR) measurements in silicon[5] have determined more than 40 independent dipolar hyperfine constants for each of the three impurities: arsenic, phosphorus, and antimony. This paper presents a calculation,[7] based on the effective-mass model, which explains the observed qualitative features for these hyperfine interactions and yields semiquantitative agreement with the experimental results.[4,5]

The anisotropic hyperfine interactions are computed as matrix elements involving the operator of the dipole-dipole interaction between a nucleus and the electron and the wave function of the impurity electron. To obtain this wave function, the standard Kohn-Luttinger approximation[1-3] is assumed, i.e., the total wave function is an appropriate ground-state sum of the degenerate valley minima wave functions, where each valley function is a slowly varying envelope function times the conduction-band minimum Bloch function of that valley.

When performing the integrations necessary to obtain the above-mentioned matrix elements, the principal difficulty lies in including the details of the Bloch function throughout the entire crystal. It is assumed that the integration over a "distant" region far away from the nucleus of interest can be performed without including the Bloch-function details since an average value over each distant unit cell of the crystal can be used. However, in the "local" region such an averaging technique is not valid and a reasonable approximation for the Bloch function must be used.

In the present paper, the Bloch function is expressed in terms of equivalent orbitals that were first used in solids by Hall.[8,9] The Bloch functions are formed by taking appropriate sums of the equivalent orbitals. The major advantage in the use of these orbitals is that the four orbitals associated with a lattice-site transform into one another under the lattice-site point-group operations T_d of the crystal. When the above symmetry requirements are combined with the symmetry properties of the dipole-dipole operator, substantial simplifications result in evaluating the local-region integrations. These integrations can then be reduced to a determination of three intrinsic crystal parameters, each parameter being multiplied by an easily evaluated

"local" coefficient which depends on the location of the conduction-band minimum in k space and on the location of the nucleus of interest relative to the impurity.

In Sec. II, the form of the total ground-state wave function is presented. In Sec. III, the theoretical expressions for the anisotropic hyperfine interactions are developed. Section IV gives a comparison of the theoretical and experimental results for the group-V impurities in silicon.

II. EFFECTIVE-MASS GROUND-STATE WAVE FUNCTION

A. Total Wave Function

The effective-mass ground-state wave function in silicon can be written as[1-3]

$$\psi(\vec{r}) = \frac{1}{\sqrt{6}} \sum_{j=1}^{6} F_j(\vec{r}) \Phi_j(\vec{r}) , \tag{1}$$

where the sum is over the six degenerate conduction-band minima – one along each of the $\langle 100 \rangle$ k-space axes; $\Phi_j(\vec{r})$ is the conduction-band Bloch function at the jth minimum and $F_j(\vec{r})$ is the slowly varying envelope function appropriate to the jth minimum.

B. Envelope Function

A form for the effective-mass envelope function is[4,6]

$$F_z(r) = F_{\rm iso}(r)(a_t^2 a_l / a^{*3})^{-1/2} \times \exp\left(-\left\{\left[(x^2+y^2)/n^2 a_t^2\right] + (z^2/n^2 a_l^2)\right\}^{1/2}\right) \times \left[\exp(-r/na^*)\right]^{-1} , \tag{2}$$

where

$$F_{\rm iso}(r) = A W_{n,1/2}(2r/n)/(2r/n) . \tag{3}$$

The above expression is for the z valleys; the x- and y-valley expressions can be obtained from symmetry considerations. In Eqs. (1) and (2), a_t, a_l, and a^* are the transverse, longitudinal, and isotropic radii[10]; A is a normalization constant for the Whittaker function $W_{n,1/2}(2r/n)$ and the index n is donor dependent[10] because of the different donor ionization energies.

C. Bloch Functions Expressed in Terms of Equivalent Orbitals

The Bloch functions can be expressed in terms of the equivalent orbitals as shown by Hall.[8,9] A typical Bloch function is

$$\Phi_k(\vec{r}) = \sum_{\alpha=1}^{4} C_\alpha(\vec{k})\, e^{i\vec{k}\cdot\vec{T}/2} \sum_m e^{i\vec{k}\cdot\vec{r}_m} \chi_\alpha^m(\vec{r}-\vec{r}_m) , \tag{4}$$

where $\chi_\alpha^m(\vec{r}-\vec{r}_m)$ is the αth equivalent orbital associated with the mth primitive cell; $\vec{r}_m$ is the vector to the corner site of the mth cell; the sum over α is a sum over the four orbitals in a given cell; the $C_\alpha(\vec{k})$ are appropriate normalization and phase constants; and the $\vec{T}_\alpha$ are translation vectors defined as

$$\begin{aligned} T_1 &= 0 , \\ T_2 &= \tfrac{1}{2}(\hat{i}+\hat{j})a , \\ T_3 &= \tfrac{1}{2}(\hat{i}+\hat{k})a , \\ T_4 &= \tfrac{1}{2}(\hat{j}+\hat{k})a , \end{aligned} \tag{5}$$

where a is the lattice constant and $\hat{i}$, $\hat{j}$, and $\hat{k}$ are unit vectors along the $\langle 100 \rangle$ directions.

Figure 1 illustrates the numbering of the four orbitals labeled by the subscript α. The orbitals are "equivalent" because (i) the four orbitals associated with a given site transform into one another when the point-group operations are applied at that site, and (ii) like-numbered orbitals in different primitive lattice cells transform into one another for the crystal-translation operations.

In addition to the "equivalence" requirements, the crystal symmetry also places restrictions on the $C_\alpha(\vec{k})$ coefficients. For example, in silicon with a conduction band of symmetry Δ_1 and for $\vec{k}$ along [100],

$$C_1 = C_4 = -C_2 = -C_3 , \tag{6}$$

with the C's independent of $|\vec{k}|$.

For the lowest conduction band in silicon, Eq. (4) may be simplified to

$$\Phi(k_x) = C_1\left(\sum_m e^{ik_0 x_m}\left[(\chi_1^m + \chi_4^m) - e^{iF/2}(\chi_2^m + \chi_3^m)\right]\right) , \tag{7}$$

where $f = \frac{1}{2}k_0 a$ and k_0 is the position of the conduction-band minimum. Similar derivations yield

$$\Phi(k_y) = C_1'\left(\sum_m e^{ik_0 y_m}\left[(\chi_1^m + \chi_3^m) - e^{iF/2}(\chi_2^m + \chi_4^m)\right]\right) \tag{8}$$

and

$$\Phi(k_z) = C_1''\left(\sum_m e^{ik_0 z_m}\left[(\chi_1^m + \chi_2^m) - e^{iF/2}(\chi_3^m + \chi_4^m)\right]\right) , \tag{9}$$

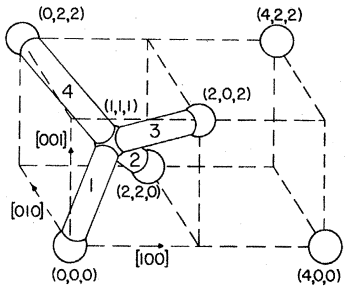

FIG. 1. Schematic illustration of the equivalent orbitals and their numbering. The primitive cell located at the donor site (0, 0, 0) is shown.

where C_1' and C_1'' are possibly different normalization constants. In the ground state each valley contributes equally to the wave function, thus

$$C_1 = C_1' = C_1'' \ . \tag{10}$$

Furthermore, let

$$C_1 = C_0 e^{i\Phi} \ , \tag{11}$$

where C_0 is a real constant and Φ will eventually be appropriately chosen.

The ground-state wave function of Eq. (1) may now be written as

$$\begin{aligned}\psi(\vec{r}) = (2C_0/\sqrt{6}) \sum_m \{ & \chi_1^m [F_x \cos(k_0 x_m + \Phi) + F_y \cos(k_0 y_m + \Phi) + F_z \cos(k_0 z_m + \Phi)] \\ & + \chi_2^m [-F_x \cos(k_0 x_m + \tfrac{1}{2} f + \Phi) - F_y \cos(k_0 y_m + \tfrac{1}{2} f + \Phi) + F_z \cos(k_0 z_m + \Phi)] \\ & + \chi_3^m [-F_x \cos(k_0 x_m + \tfrac{1}{2} f + \Phi) + F_y \cos(k_0 y_m + \Phi) - F_z \cos(k_0 z_m + \tfrac{1}{2} f + \Phi)] \\ & + \chi_4^m [F_x \cos(k_0 x_m + \Phi) - F_y \cos(k_0 y_m + \tfrac{1}{2} f + \Phi) - F_z \cos(k_0 z_m + \tfrac{1}{2} f + \Phi)] \} \ ,\end{aligned} \tag{12}$$

where the orbitals are considered to be real. For brevity of notation it is convenient to rewrite this equation as

$$\psi(\vec{r}) = (2C_0/\sqrt{6}) \times \sum_m (W_1^m \chi_1^m + W_2^m \chi_2^m + W_3^m \chi_3^m + W_4^m \chi_4^m) \ , \tag{13}$$

where the W_α^m coefficients are defined by Eqs. (12) and (13).

It is convenient to visualize the equivalent orbitals as similar to bonding and antibonding molecular orbitals between lattice sites for the valence and conduction bands, respectively. However, the application of equivalent orbitals to solids has been criticized[11,12] and Hall[9] has commented on the criticism. Part of the criticism seems to be based on the association of equivalent orbitals with molecular orbitals formed by a linear combination of atomic orbitals (MO-LCAO). Indeed, the MO-LCAO representation has been used in the few applications[13] of equivalent orbitals in the literature. However, we shall avoid a detailed representation of the equivalent orbitals (expect for order-of-magnitude estimates) and we shall formulate the theory in terms of a few constants to be fit to the experimental data.[14] Such an approach is not inconsistent with other widely used band theories, such as pseudopotentials[15] and LCAO's,[16] which also use adjustable parameters.

Although we shall not use a detailed expression for the equivalent orbitals in this paper, we believe that it may be possible to calculate such orbitals. Indeed, a procedure for just such a calculation may have already appeared in the literature. Anderson[17] has proposed a pseudopotential method for calculating "ultralocalized functions" for energy bands. These "ultralocalized functions" seem to us to be similar to, and possibly identical with, the equivalent orbitals of Hall.

III. CALCULATION OF ANISOTROPIC HYPERFINE INTERACTIONS

A. Anisotropic Tensor

The anisotropic part of the hyperfine tensor may be written as

$$\overleftrightarrow{B} = g g_N \mu_B \mu_N \langle \psi | \overleftrightarrow{D} | \psi \rangle \ , \tag{14}$$

where the magnetic constants are defined in the standard manner; $\psi(\vec{r})$ is the the wave function of the unpaired electron; and $\overleftrightarrow{D}$ is the dipole-dipole tensor operator whose components are

$$D_{ij} = (3 x_i x_j - r^2 \delta_{ij})/r^5 \ , \tag{15}$$

where r is measured from the nuclear site of interest; x_i represents x, y, or z for $i = 1$, 2, or 3, respectively; and δ_{ij} is the Kronecker δ function. It is convenient to consider the tensor expressed in the cubic-crystal-axes coordinate system. The x, y, z axes are measured from an origin located at the nucleus on the lattice site of interest. The coordinate system centered on the donor will be designated by a subscripted d, e.g., $\vec{r}_d$. The lattice-site coordinates (n_1, n_2, n_3) will be designated in the standard manner as shown in Fig. 2. The dipole-dipole tensor for nuclei in the first and third quadrants of the $(\bar{1}10)$ plane will be computed, i.e., those lattice sites with coordinates $n_1 = n_2$. Inspection of Eqs. (14) and (15) shows that

$$\sum_{i=1}^{3} B_{ii} = 0 \tag{16}$$

and

$$B_{ij} = B_{ji} \ , \tag{17}$$

and, furthermore, for sites with $n_1 = n_2$,

$$B_{xz} = B_{yz} \quad \text{and} \quad B_{xx} = B_{yy} \ . \tag{18}$$

As a consequence of Eqs. (16)–(18), the dipole tensor for any nucleus under consideration can be

expressed by at most three independent components which are chosen as B_{zz}, B_{xy}, and B_{xz}.

The anisotropic hyperfine tensors are given by Eqs. (14) and (15), with ψ given in Eq. (13). Therefore,

$$B_{ij} = (\tfrac{1}{3} 2gg_n \mu_B \mu_N |C_0|^2) \sum_{l,m,\alpha,\mu} \langle W_\alpha^l \chi_\alpha^l | D_{ij} | W_\mu^m \chi_\mu^m \rangle , \tag{19}$$

where the summations over l and m run over the entire lattice. The above equation will be evaluated by dividing the problem into a local and a distant contribution.

B. Distant Contributions

If the integration in Eq. (14) is considered as a summation over all primitive cells of integrations over each cell, then it is clear that the details of the Bloch function within the cell are unimportant for cells so distant from the nuclear site of interest that D_{ij} varies little over the cell. Also, the effective-mass theory assumes that the envelope function F_j [see Eqs. (1) and (2)] is slowly varying over a primitive cell. Therefore, using the approximations that F_j and D_{ij} are slowly varying for distant cells and using the orthonormality properties of the Bloch function one obtains

$$B_{ij}(\text{distant}) = \tfrac{1}{3} gg_n \mu_B \mu_N \sum_{m=1}^{3} \langle F_m | D_{ij}' | F_m \rangle , \tag{20}$$

where we have now replaced the sum over all primitive cells of $F_m^2 D_{ij}$ by an integration over the entire "distant" region. In calculating the above, we have found the distant contribution to be only a small percentage of the total dipole interaction. To save computer time, we have thus used only the isotropic part of the envelope function, so that

$$B_{ij}(\text{distant}) = gg_n \mu_B \mu_N \langle F_{\text{iso}} | D_{ij} | F_{\text{iso}} \rangle . \tag{21}$$

In the central-cell region, centered on the donor, F_{iso} is not slowly varying and thus Eq. (21) might not be valid. Therefore, we have considered this region in detail[18] and have concluded that the central-cell region contributes only a small fraction to B_{ij} (distant) and can be well enough estimated by extending the integration in Eq. (21) over this region.

In addition, we have found that the integration in Eq. (21) is insensitive to the position of the boundary between the local region centered on the nucleus of interest and the distant region provided the local region is less than two primitive-cell volumes.[18] Thus, we have calculated B_{ij} (distant) by performing the integration in Eq. (21) over the entire crystal. Table I shows the results of our distant calculations for a few sites for the different donors in silicon. Table II shows a more extensive list of sites for an arsenic donor. Note that the distant contribution is small compared to the experimental values given in parentheses.

TABLE I. Typical distant dipole interactions for different donors. The interactions vary with donor as shown because of properties of the donor-dependent envelope function. The symbol * means the value is zero by symmetry. The symbol ** means the calculated value is zero but is not required by symmetry.

Site	Donor	B_{zz} (kHz)	B_{xy} (kHz)	B_{xz} (kHz)
(0, 0, 4)	As	13.1	**	*
	P	.7.5	**	*
	Sb	6.6	**	*
(3, 3, 3)	As	*	4.1	B_{xy}
	P	*	2.7	B_{xy}
	Sb	*	2.2	B_{xy}
(4, 4, 0)	As	− 3.7	5.5	**
	P	− 2.4	3.7	**
	Sb	− 2.0	3.1	**

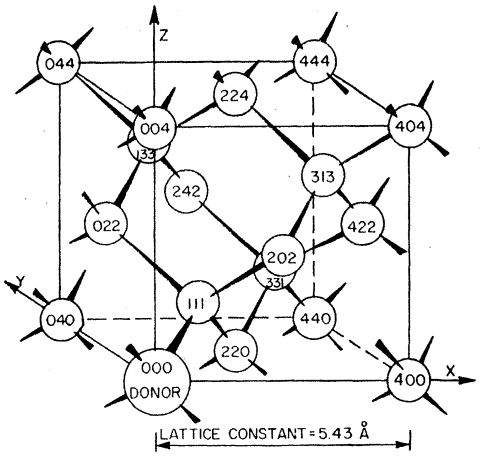

FIG. 2. Tetrahedral lattice with donor at coordinate origin. The figure shows 17 neighboring nuclei which are members of seven different shells. The dipole tensors are expressed with reference to the x, y, and z directions shown in the figure.

C. Local Contribution

1. *Approximations*

In evaluating the local contribution using Eq. (19), we have restricted the calculations to the four equivalent orbitals associated with the particular lattice site of interest at R_l, i.e., we neglect the contributions of next-nearest and more-distant χ's. We believe this is a valid approximation for several reasons. If the contributions of next-nearest orbitals are estimated[18] using an sp^3 hybrid approximation for the χ's, then the contributions are small

TABLE II. Distant dipole interactions for various sites about an arsenic impurity. Sites are grouped into various classes for ease of comparison with experimental data. Values in parentheses are *total* experimental values based on site correlations using the Fermi contact interactions. Inversion-related sites have the same distant interaction in this approximation. The symbol * means the value is zero by symmetry. The symbol ** means the value is zero but not required by symmetry.

Class	Site	B_{zz} (kHz)	B_{xy} (kHz)	B_{xz} (kHz)
[001]	(0, 0, 4)	13.1 (57.0)	** (±55.8)	*
axis	(0, 0, 8)	5.4 (16.0)	** (±7.6)	*
class	(0, 0, 12)	2.9	**	*
[111]	$(\bar{1}, 1, 1)$	*	17 (1258)	B_{xy}
axis	$(\bar{3}, \bar{3}, \bar{3})$	*	4.1	B_{xy}
class	(4, 4, 4)	*	3.0	B_{xy}
	(5, 5, 5)	*	2.3	B_{xy}
(110)	(2, 2, 0)	−9.0	13.4	**
plane	$(\bar{1}, \bar{1}, \bar{3})$	10.8	2.0	6.0
class	(3, 3, 1)	−4.4	7.3	2.5
	(2, 2, 4)	5.1	2.5	4.8
	(1, 1, 5)	9.0	0.6	1.5
	(4, 4, 0)	−3.7 (−41.6)	5.5 (148.2)	** (72.2)
	(3, 3, 5)	2.6	2.2	3.6
	(5, 5, 1)	−2.7	4.1	0.8
	(6, 6, 0)	−2.2	3.7	**
	$(\bar{1}, \bar{1}, \bar{7})$	5.8	0.3	0.4
	$(\bar{5}, \bar{5}, \bar{3})$	−1.4	3.2	1.9
	$(\bar{3}, \bar{3}, \bar{7})$	2.9	1.0	2.3

compared to the contributions of the nearest orbitals. Also, recent calculations[19] have compared equivalent orbital results with dipolar calculations using pseudopotential Bloch functions. These comparisons show that the nearest-equivalent-orbital approximation of the Bloch function is probably better than the effective-mass-theory approximation of the shallow donors.

A further simplification can be made in evaluating the local integrals in Eq. (19). Namely, since $F(\vec{r})$ is a slowly varying function over a unit cell (the effective-mass theory assumes this), $F(\vec{r})$ can be assumed to have the value $F(\vec{R}_l)$ near the $\vec{R}_l$ lattice site. This approximation can be considered as the first term in a Taylor series expansion of $F(\vec{r})$ about $\vec{R}_l$. Detailed estimates[18] of the second- and higher-order Taylor series terms show that they are even less important than the contribution of the more-distant equivalent orbitals mentioned above.

2. *Reduction of Local Interaction to Three Intrinsic Parameters*

According to the above discussion, the "local" part of the dipole interaction will be restricted to those terms in the summation over l, n, α, μ in Eq. (19) that correspond to the four equivalent orbitals associated with the lattice site of interest. For each B_{ij} term one obtains 16 integrals of the form

$$I_{ij}(\alpha, \mu) = \tfrac{1}{3} 2 C_0^2 g g_n \mu_B \mu_n \langle \chi_\alpha | D_{ij} | \chi_\mu \rangle , \tag{22}$$

where, clearly,

$$I_{ij}(\alpha, \mu) = I_{ij}(\mu, \alpha) , \tag{23}$$

since D and the χ's are real. The tetrahedral equivalence of the orbitals permits other simplifications and was one of the motivating reasons for using the equivalent orbitals. Thus for the D_{zz} integrals, Appendix A shows

$$I_{zz}(\alpha, \alpha) = 0 , \tag{24}$$

$$I_{zz}(1, 3) = I_{zz}(1, 4) = I_{zz}(2, 3) = I_{zz}(2, 4) = -\tfrac{1}{2} I_{zz}(1, 2) , \tag{25}$$

and

$$I_{zz}(3, 4) = I_{zz}(1, 2) . \tag{26}$$

These results show that all the D_{zz} integrals can be expressed in terms of one *intrinsic* parameter which is chosen as $I_{zz}(1, 2)$ and will hereafter be referred to as simply I_{zz}. For the D_{xy} integrals,

$$I_{xy}(2, 2) = -I_{xy}(3, 3) = -I_{xy}(4, 4) = I_{xy}(1, 1) , \tag{27}$$

$$I_{xy}(3, 4) = -I_{xy}(1, 2) , \tag{28}$$

and

$$I_{xy}(1, 3) = I_{xy}(1, 4) = I_{xy}(2, 3) = I_{xy}(2, 4) = 0 . \tag{29}$$

For the D_{xz} integrals,

$$I_{xz}(1, 1) = I_{xy}(1, 1) , \tag{30}$$

$$I_{xz}(2, 2) = -I_{xz}(3, 3) = I_{xz}(4, 4) = -I_{xy}(1, 1) , \tag{31}$$

$$I_{xz}(1, 2) = I_{xz}(1, 4) = I_{xz}(2, 3) = I_{xz}(3, 4) = 0 , \tag{32}$$

and finally,

$$I_{xz}(1, 3) = -I_{xz}(2, 4) = I_{xy}(1, 2) . \tag{33}$$

The results are that all the D_{xy} and D_{xz} integrals can be expressed in terms of two *intrinsic* parameters which we have chosen as $I_{xy}(1, 1)$ and $I_{xy}(1, 2)$ and which will hereafter be referred to as simply I_1 and I_2, respectively.

Thus, the many integrals in the local interaction have been reduced to three intrinsic integrals, I_{zz}, I_1, and I_2. In general, these three integrals are independent, but for an oversimplified model they can be shown to be related. Possible relationships between the three integrals are discussed in Appendix B.

3. *Final Derivation of Local Contribution*

Before the local contributions to the dipole tensor can be evaluated, it is necessary to know the values of k_0 and Φ that appear in Eq. (12). The term Φ was introduced in Eq. (11), and it determines the

phase of the Bloch function [Eqs. (7)–(9)]. The linear combination of Bloch functions given in Eq. (1) as the ground state assumes that the Bloch functions are phased to be real at the donor site. We shall assume that only the four equivalent orbitals associated with the donor site contributed to the Bloch function at this site, i.e., we neglect any contributions from more distant orbitals. This approximation in the determination of Φ seems to be consistent with the neglect of distant orbitals in the evaluation of the local part of the dipole interaction discussed above. These considerations lead to

$$\Phi = \tfrac{1}{4}f - \tfrac{1}{2}\pi \quad . \tag{34}$$

The location[20] of the conduction-band minimum in silicon is on the Δ_1 axis, between 80% and 90% of the distance to the X point, i.e., $0.8 < ak/2\pi < 0.9$. Because of this uncertainty in k_0, we have calculated the B tensors for several values of k_0. Thus the final theoretical predictions will be given as a range of values corresponding to the above range of k_0.

Equation (12) is expressed in terms of $\vec{r}_m$, the corner positions of the primitive cells of the lattice. However, it is desirable to express the final theoretical B (local) values in terms of the lattice site positions $\vec{R}_m$. This change may be made for the a sites, the odd-numbered lattice sites, by the substitution $\vec{r}_m = \vec{R}_m - \frac{1}{4}(\hat{i}+\hat{j}+\hat{k})a_0$. For the b or even-numbered sites, $\vec{R}_m$ is the same as $\vec{r}_m$. However, when Eq. (13) is substituted into Eq. (19) and only the χ_α's associated with the b sites are retained from the summation over l and m, it must be kept in mind that the four χ_α's associated with the b sites come from four different primitive cells with origins located at $\vec{r}_m = \vec{R}_l - \vec{T}_\alpha$.

We now write the final expression for the local contribution[21]:

$$B_{zz}(\text{local}) = W_{zz} I_{zz} \ , \tag{35}$$

$$B_{xy}(\text{local}) = W_{y1} I_1 + W_{y2} I_2 \ , \tag{36}$$

$$B_{xz}(\text{local}) = W_{z1} I_1 + W_{z2} I_2 \ , \tag{37}$$

where

$$W_{zz} = 2W_1 W_2 + 2W_3 W_4 - W_1 W_3 - W_1 W_4 - W_2 W_3 - W_2 W_4 \ , \tag{38}$$

$$W_{y1} = W_1^2 + W_2^2 - W_3^2 - W_4^2 \ , \tag{39}$$

$$W_{y2} = 2(W_1 W_2 - W_3 W_4) \ , \tag{40}$$

$$W_{z1} = W_1^2 - W_2^2 + W_3^2 - W_4^2 \ , \tag{41}$$

$$W_{z2} = 2(W_1 W_3 - W_2 W_4) \ , \tag{42}$$

and

$$W_1 = F_x C_x^+ + F_y C_y^+ + F_z C_z^+ \ , \tag{43}$$

$$W_2 = -F_x C_x^- - F_y C_y^- + F_z C_z^+ \ , \tag{44}$$

$$W_3 = -F_x C_x^- + F_y C_y^+ - F_z C_z^- \ , \tag{45}$$

$$W_4 = F_x C_x^+ - F_y C_y^- - F_z C_z^- \ , \tag{46}$$

and

$$C_x^\pm = \cos(k_0 X_l - \tfrac{1}{2}\pi \pm \tfrac{1}{4}f) \ . \tag{47}$$

The above results are for the b (even-numbered) sites, the corresponding results for the a (odd-numbered) sites are obtained by interchanging the + and − superscripts of the C coefficient in Eqs. (43)–(46). The F_i envelope functions in Eqs. (43)–(46) are to be evaluated at the corresponding lattice site R_l.

Considering the complexity of the problem, the relative simplicity of the above equations for the local dipolar hyperfine integration should not be overlooked. The three parameters I_{zz}, I_1, and I_2 are intrinsic parameters that depend only on the host lattice and are independent of donor. The five W factors are the parameters which depend on the donor impurity through the envelope function and on the location of the nuclear site of interest through the envelope function and cosine functions. In addition, the W parameters depend also on the host lattice through the location of the conduction-band minimum k_0.

To complete the local-region calculations, values for the intrinsic parameters must be obtained. Ideally, these could be calculated from first principles using Eq. (22); however, an accurate detailed form for the equivalent orbitals is not known at this time. Therefore, we shall obtain the integral parameters by fitting to the experimental values. In the present case, we shall use three independent experimentally measured anisotropic hyperfine constants and then attempt to predict the more than 100 other experimental constants for the three common group-V donor impurities in silicon.

IV. EXPERIMENTAL RESULTS AND THEORETICAL PREDICTIONS

A. Review of Experimental Results

The most recent and complete data on the shallow-donor hyperfine interactions are given in Ref. 5. Table III lists the experimental hyperfine constants in a form that is convenient for comparison with the theoretical predictions. In addition to the values of the constants, the experimental results also give the symmetry class to which a shell belongs. The shells A and K must be associated with a $\langle 001 \rangle$ axis class. The shells C, E, H, J, O, and N must be associated with a $\langle 111 \rangle$ axis class. The remaining shells must be associated with a $\{110\}$ plane class but not along either the $\langle 001 \rangle$ or $\langle 111 \rangle$ axes.

Considerable difficulties occur when an attempt is made to assign the experimental shells to specific lattice sites (see Ref. 6 for a discussion of these difficulties). One motivation for the present

TABLE III. Experimental hyperfine interactions. All values are in kHz. Absolute value signs occur because the signs cannot be determined by ENDOR. The symbol * means that the value is zero by symmetry. The experimental error is typically ±1 or 2 kHz. The values are taken from Ref. 5.

Shell class	Donor	$\lvert\frac{1}{2}a\rvert$	B_{zz}	B_{xy}	$\lvert B_{xz}\rvert$
A	As	3860	57.0	| 55.8 |	0*
⟨001⟩	P	2981	41.4	| 41.4 |	0*
axis	Sb	3101	46.0	| 34.2 |	0*
B	As	3000	−41.6	148.2	72.2
{110}	P	2254	−34.0	106.2	39.8
plane	Sb	1833	−28.6	79.2	20.2
C	As	2037	0*	5.8	B_{xy}
⟨111⟩	P	1649	0*	5.0	B_{xy}
axis	Sb	1397	0*	6.0	B_{xy}
D	As	1292	4.2	20.4	25.4
{110}	P	1117	3.6	16.6	22.2
plane	Sb	1003	0.0	17.4	17.4
E	As	642	0*	1258	B_{xy}
⟨111⟩	P	270	0*	700	B_{xy}
axis	Sb	293	0*	522	B_{xy}
F	As	1121	151.0	−41.2	4.6
{110}	P	840	116.4	−28.2	11.8
plane					
G	As	806	7.0	− 1.0	5.6
{110}	P	764	5.0	− 1.2	5.0
plane	Sb	761	4.6	− 1.2	5.2
H	As	801	0*	62.4	B_{xy}
⟨111⟩	P	689	0*	50.6	B_{xy}
axis	Sb	703	0*	44.6	B_{xy}
I	As	718	−20.4	31.8	12.0
{110}	P	685	−17.4	27.8	13.8
plane	Sb	643	−14.0	22.6	14.4
J	As	694	0*	<5	B_{xy}
⟨111⟩	P	739	0*	5.4	B_{xy}
axis					
K	As	758	16.0	| 7.6 |	0*
⟨001⟩	P	663	14	< | 12 |	0*
axis					
L	As	741	−14.6	9.8	8.2
{110}	P	582	−11.2	2.6	7.6
plane	Sb	425	− 5.8	3.8	4.4
M	As	777	−60.8	65.2	41.4
{110}	P	612	−40.6	49.6	35.6
plane	Sb	559	−37.2	44.0	30.6
N	As	607	0*	4.2	B_{xy}
⟨111⟩	P	612	0*	3.4	B_{xy}
axis					
O	As	739	0*	35.8	B_{xy}
⟨111⟩	P	598	0*	32.6	B_{xy}
axis	Sb	670	0*	31.4	B_{xy}
P	As	696	− 4.8	0.4	4.2
{110}	P	662	− 6	<6	<6
plane	Sb	629	− 5.8	− 4.6	4.8

TABLE III. (*continued*)

Shell class	Donor	$\lvert\frac{1}{2}a\rvert$	B_{zz}	B_{xy}	$\lvert B_{xz}\rvert$
Q	As	566	−48.0	101.6	27.6
{110}	P	524	−40.2	84.0	22.8
plane	Sb	387	−36.0	78.6	31.6
R	As	428	24.8	0.0	25.0
{110}	P	379	21.0	0.2	19.4
plane	Sb	332	15.0	−2.8	12.0
S	As	377	− 5.4	9.2	0.0
{110}	P	410	− 5.4	7.4	0.0
plane					
T	As	364	0.0	4.4	4.4
{110}	P	398	0.0	3.8	4.2
plane					
X	As	242	40	30	•••
{110}	P	317	29.4	23.6	32.2
plane	Sb	437	20.4	19.0	20.8

calculation was to assist in this assignment. At first it seems somewhat surprising that the largest Fermi contact interaction (shell *A*) or wave-function density must occur at the fourth (0, 0, 4), twenty-second (0, 0, 8), or more remote neighbor shell; however, the effective-mass theory predicts that the (0, 0, 4) site is expected to have the largest wave-function density.[4,6] Thus, because of the remoteness of all the other ⟨001⟩ axis shells and because of the theoretical prediction, there is no doubt that shell *A* is the (0, 0, 4) shell. Similar arguments strongly suggest that shell *K* is the (0, 0, 8). Contact calculations suggest that the group of six observed ⟨111⟩ axis-class shells is contained in the group of lattice shells (1, 1, 1), $(\bar{3}, \bar{3}, \bar{3})$, (4, 4, 4), $(\bar{4}, \bar{4}, \bar{4})$, (5, 5, 5), and $(\bar{7}, \bar{7}, \bar{7})$. The quite large dipolar constant for shell *E* indicates that it is the (1, 1, 1) nearest-neighbor shell. The contact calculations slightly favor shell *C* as the $(\bar{3}, \bar{3}, \bar{3})$ shell, but this is not certain and the remaining ⟨111⟩ axis-shell assignments are not known from contact-interaction considerations.

The majority of the experimental and nearby lattice shells are of the {110} plane class. The contact calculations strongly suggest that shell *B* is the (4, 4, 0) shell. They suggest no other specific assignments but they do restrict, to some extent, the possible lattice sites to which an experimental shell can be assigned. Based on the above assignments, the three intrinsic parameters will be chosen and predictions will be made for the other shell dipolar constants.

B. Predictions for B_{zz} Dipolar Constants

The equation used to predict the B_{zz} dipolar constants is

$$B_{zz}(\text{theory}) = B_{zz}(\text{distant}) + B_{zz}(\text{local}) , \quad (48)$$

where B_{zz}(distant) is computed from Eq. (21) with typical values given in Tables I and II; B_{zz}(local) can be computed using Eq. (35) once I_{zz} is obtained by a fitting procedure. The most reliably known B_{zz} constant is that for shell A, the (0, 0, 4) shell. Thus, from this constant, I_{zz} may be obtained as

$$I_{zz}(k_0) = [B_{zz}(\text{exp}) - B_{zz}(\text{distant})] / W_{zz}(k_0) \quad (49)$$

for the (0, 0, 4) shell. To evaluate Eq. (49), a specific donor must be chosen. The dipolar constants and ENDOR signals are largest in arsenic and thus these constants have the smallest percent error. Furthermore, the arsenic spectrum has been studied in greatest detail. For these reasons, I_{zz} is evaluated using the arsenic data and the results are used for the other donors. Table IV contains the results for I_{zz} using Eq. (49) and various assumed values of k_0.

C. Predictions for B_{xy} and B_{xz} Dipolar Constants

The B_{xy} and B_{xz} dipolar constants have been calculated together since the two intrinsic parameters I_1 and I_2, necessary to predict B_{xy}, must also be used to predict B_{xz} [see Eqs. (36) and (37)]. There are several known values which may be used to obtain I_1 and I_2 such as $B_{xy}(1, 1, 1)$, $B_{xy}(0, 0, 4)$, $B_{xy}(4, 4, 0)$, $B_{xz}(4, 4, 0)$, and $B_{xy}(0, 0, 8)$. The first of these values we are reluctant to use because several of the approximations in the theory could possibly be very poorly satisfied for the nearest-neighbor shell. Unfortunately, there exists no choice of I_1 and I_2 which is completely compatible with the other dipolar constants. The most disturbing incompatibility is that of $B_{xy}(0, 0, 4)$ and $B_{xz}(4, 4, 0)$. Since, for the local contribution,

$$B_{xy}(0, 0, 4) = W_{y1}(0, 0, 4)(I_1 + I_2) \quad (50)$$

and

$$B_{xz}(4, 4, 0) = W_{z1}(4, 4, 0)(I_1 + I_2) \quad (51)$$

for all three donors, the following result should be valid for the local contribution:

$$B_{xy}(0, 0, 4)/B_{xz}(4, 4, 0) = W_{y1}(0, 0, 4)/W_{z1}(4, 4, 0) \approx 2 \mp \tfrac{1}{3} \quad (52)$$

TABLE IV. Fitted values for the integral parameters. [See Eqs. (49), (50), and (54).]

k_0/k_{max}	0.80	0.83	0.85	0.86	0.89
$I_{zz}(k_0)$	1.37	1.67	2.01	2.25	3.40
$I_1(k_0)$	3.89	4.66	5.54	6.15	9.20
$I_2(k_0)$	−3.07	−3.84	−4.69	−5.27	−8.20

and the $\mp\frac{1}{3}$ is due to the uncertainty in k_0. The measured ratios for the different donors varies from about $|\frac{3}{4}|$ to $|1\frac{3}{4}|$. These measured ratios and the ratio of Eq. (52) should all be equal since the distant calculations for the two dipolar constants of interest are zero. The conclusion we draw from this discrepancy is that a factor of 2 or 3 uncertainty will have to be tolerated in the numerical calculations of the dipolar constants at present, as is also the case for the Fermi contact calculations.[6]

The ratio

$$B_{xy}(0, 0, 4)/B_{xy}(0, 0, 8) = W_{y1}(0, 0, 4)/W_{y1}(0, 0, 8) \quad (53)$$

can be matched to the experimental ratio. We have chosen, however, not to use the $B_{xy}(0, 0, 8)$ value for fitting because of its strong k_0 dependence.

Another expression for I_1 and I_2 is obtained from B_{xy} for the (4, 4, 0) shell:

$$I_1 - I_2 = [B_{xy}(\text{exp}) - B_{xy}(\text{distant})]/W_{y1} \quad (54)$$

After considerable study of these relationships, as well as others concerned with the ⟨111⟩ axes-class shells, the choice of I_1 and I_2 has been determined by using Eqs. (50) and (54). In addition, since the sign of the experimental value of B_{xy} for the (0, 0, 4) shell is not known, we assume this value as negative, based on recent calculations.[19] This fit gives the values of I_1 and I_2 presented in Table IV.

D. Comparison of Experiment and Theory

All of the B_{xy}, B_{xz}, and B_{zz} constants can now be calculated. Table V shows the comparison of calculated and experimental values for the three shallow donors for the few sites that can be definitely identified. The agreements for the dipole constants are as good as for experimental and theoretical Fermi contact interactions.[6]

The predictions for other sites which are as yet uncorrelated with the experimental data are given in Table VI. Ideally, it should be possible to assign all experimental shells to actual lattice shells on the basis of the predictions presented in Table VI; however, as discussed above, discrepancies occurred in the fitting procedure even before the predictions were evaluated. Thus the predictions must be considered as having only qualitative accuracy. Despite this limitation, a number of worthwhile features concerned with the shell assignments have been revealed by the calculations.

One feature is the additional confirmation of shell K as the (0, 0, 8) shell – not only because of the exclusion of the (0, 0, 12) and more remote shells – but also because of the actual B_{zz} and B_{xy} predicted values. The predictions also confirm shell E to be the (1, 1, 1) shell since it is (i) predicted to have an order of magnitude larger dipolar constant than any other shell and (ii) the predicted

TABLE V. Comparison of the total dipolar constants (in kHz). The three * values were used for fitting. The first number refers to $k_0 = 2\pi(0.85)/a$. The upper sign is for $k_0 = 2\pi(0.80)/a$ and the lower for $k_0 = 2\pi(0.90)/a$.

		As	P	Sb
Site (0, 0, 4)				
	Calc	*	43 ± 1	39 ± 1
B_{zz}	Exp	57	$41\frac{1}{2}$	46
	Calc	*	-46 ± 0	-40 ± 0
B_{xy}	Exp	$\lvert 56 \rvert$	$\lvert 41\frac{1}{2} \rvert$	$\lvert 34 \rvert$
Site (0, 0, 8)				
	Calc	18 ∓ 9	15 ∓ 9	14 ∓ 8
B_{zz}	Exp	16	14	•••
	Calc	-12 ± 6	-12 ± 6	-11 ± 6
B_{xy}	Exp	$\lvert 7\frac{1}{2} \rvert$	$< \lvert 12 \rvert$	•••
Site (4, 4, 0)				
	Calc	-32 ± 0	-28 ± 0	-25 ± 0
B_{zz}	Exp	$-41\frac{1}{2}$	-34	$-28\frac{1}{2}$
	Calc	*	130 ± 0	115 ± 0
B_{xy}	Exp	148	160	79
	Calc	-27 ± 4	-24 ± 4	-22 ± 4
B_{xz}	Exp	$\lvert 72 \rvert$	$\lvert 40 \rvert$	$\lvert 20 \rvert$
Site (1, 1, 1)				
	Calc	1500 ∓ 700	1000 ∓ 500	850 ∓ 400
B_{xy}	Exp	1260	700	520

value of this constant is reasonably correct. The prediction of Table VI, when used in conjunction with the Fermi contact calculations, strongly suggests shells H and O are to be chosen from the $(\bar{3}, \bar{3}, \bar{3})$, $(4, 4, 4)$, and $(\bar{4}, \bar{4}, \bar{4})$ lattice shells.

Some of the lattice shells are related by inversion. Examples of these are $(4, 4, 4)$ and $(\bar{4}, \bar{4}, \bar{4})$, $(8, 8, 8)$ and $(\bar{8}, \bar{8}, \bar{8})$, $(2, 2, 4)$ and $(\bar{2}, \bar{2}, \bar{4})$, and $(2, 2, 8)$ and $(\bar{2}, \bar{2}, \bar{8})$. Because of the approximations made in obtaining the effective-mass envelope functions, the Fermi contact constants and the B_{zz} constants are predicted to be equal for the inversion-related shells. However, inversion is not a symmetry of the shallow-donor problem and the experimental results show no such features. On the other hand, even with the approximations made, the B_{xy} and B_{yz} constants are *not* equal (see Table VI) for inversion-related sites.

There are two other general features of the theoretical values that agree with the experimental results: (i) The magnitude of the B_{ij} values for a given site varies from donor to donor in the same way that the Fermi contact constant varies, i.e., through the donor dependence of the envelope function. (ii) For a given lattice site, the magnitudes of the Fermi contact constant and the three B_{ij} values are seemingly uncorrelated because the interference effects between the cosine terms are different for all four hyperfine constants.

In addition to the discrepancy discussed in connection with Eq. (52), there is another feature of the experimental results that is not explained by our dipole theory. Shell F has large negative values of B_{xy} (see Table III) and none of the values predicted in Table VI have this feature.

V. CONCLUSIONS

A theory has been developed for the anisotropic (dipolar) hyperfine constants of lattice nuclei interacting with a shallow-donor electron that is described by the effective-mass approximation. When applied to the ground state of the shallow donors in silicon, the basic features of the experimental results can be qualitatively and semiquantitatively understood for the first time. However, it is not possible at this time to assign all of the experimental shells to definite lattice sites using both the Fermi contact and the B_{ij} values. We believe that this is due to the inadequacy of the effective-mass

TABLE VI. Theoretical predictions of the B_{ij} values for the arsenic donor. Three numbers are given for each B_{ij}. The first number refers to $k_0\, a/2\pi = 0.85$, the upper sign refers to $k_0\, a/2\pi = 0.80$, and the lower sign refers to $k_0\, a/2\pi = 0.90$. The theoretical values are based on fitting to the three starred (*) values.

Site	$(0,0,4)$	$(0,0,8)$	$(0,0,12)$	$(1,1,1)$	$(\bar{3},\bar{3},\bar{3})$	$(4,4,4)$	$(\bar{4},\bar{4},\bar{4})$	$(5,5,5)$	$(\bar{7},\bar{7},\bar{7})$
B_{zz}	57.0^*	18 ∓ 9	5 ∓ 2	0	0	0	0	0	0
B_{xy}	-55.8^*	-12 ± 6	-1 ± 3	1500 ∓ 700	200 ∓ 150	95 ± 6	125 ∓ 7	$10 \mp \frac{8}{50}$	1 ± 8
B_{xz}	0	0	0	B_{xy}	B_{xy}	B_{xy}	B_{xy}	B_{xy}	B_{xy}
Site	$(8,8,8)$	$(\bar{8},\bar{8},\bar{8})$	$(2,2,0)$	$(\bar{1},\bar{1},\bar{3})$	$(3,3,1)$	$(2,2,4)$	$(\bar{2},\bar{2},\bar{4})$	$(1,1,5)$	$(4,4,0)$
B_{zz}	0	0	-40 ∓ 5	-60 ± 15	41 ∓ 8	24 ∓ 2	24 ∓ 2	-54 ± 18	-32 ± 0
B_{xy}	25 ∓ 15	22 ∓ 20	165 ± 30	650 ∓ 250	250 ∓ 150	95 ± 20	55 ± 10	320 ∓ 150	148.2^*
B_{xz}	B_{xy}	B_{xy}	-15 ∓ 1	-450 ± 250	-320 ± 150	-120 ∓ 15	-95 ∓ 8	75 ∓ 100	-27 ± 4
Site	$(3,3,5)$	$(5,5,1)$	$(\bar{1},\bar{1},\bar{7})$	$(\bar{5},\bar{5},\bar{3})$	$(\bar{3},\bar{3},\bar{7})$	$(6,6,0)$	$(2,2,8)$	$(\bar{2},\bar{2},\bar{8})$	$(8,8,0)$
B_{zz}	-17 ± 9	33 ∓ 10	-35 ± 20	12 ∓ 7	-14 ± 15	-18 ± 5	6 ∓ 9	6 ∓ 9	-8 ± 5
B_{xy}	120 ∓ 80	0 ∓ 25	200 ∓ 100	10 ∓ 30	80 ∓ 50	85 ∓ 30	40 ± 2	18 ± 10	35 ∓ 25
B_{xz}	-50 ± 50	60 ∓ 60	10 ± 50	-36 ± 40	10 ∓ 30	6 ± 5	-45 ± 10	-30 ± 20	-2 ± 2

approximation in accurately describing the ground states of the shallow donors.[22]

The theory presented in this paper is based on the equivalent-orbital formulation. The theory requires only three constants I_{zz}, I_1, and I_2 to explain a large number of experimental results. We are well aware that the dipole theory could also be formulated in terms of a LCAO or a Wannier-function representation of the Bloch functions. Also, it is possible to extend the theory to next-nearest equivalent orbitals. However, recent calculations[19] using pseudopotential Bloch functions have shown that the equivalent orbitals give surprisingly good fits with just the three constants. We believe that any improvement in the theoretical hyperfine constants must wait for better ground-state wave functions for the shallow donors.

APPENDIX A: PROOF OF SOME INTEGRAL RELATIONSHIPS

The proofs of Eqs. (24)–(33) are based on the symmetry properties of the equivalent orbitals and the operators involved in the integrals as discussed below. Equation (24) can be proven by observing that

$$\langle\chi_\alpha|\, z^2/r^5|\,\chi_\alpha\rangle = \langle\chi_\alpha|\, x^2/r^5|\,\chi_\alpha\rangle = \langle\chi_\alpha|\, y^2/r^5|\,\chi_\alpha\rangle\ .$$

Thus,

$$I_{zz}(\alpha,\alpha) \equiv \langle\chi_\alpha|\, 3z^2 - r^2/r^5|\,\chi_\alpha\rangle \equiv 0\ .$$

To prove Eq. (25), it is noted that all but the last equality follow by a careful consideration of Fig. 1, where, with site (1, 1, 1) as an origin, the directions $-y$, $-x$, $+x$, and $+y$, respectively, are indistinguishable for the four respective integrations of Eq. (25). The last equality follows because the first four integrals are equivalent to $I_{xx}(1,2) = I_{yy}(1,2)$ as essentially explained above; but

$$I_{xx}(1,2) + I_{yy}(1,2) + I_{zz}(1,2) \equiv 0\ ,$$

since we know the diagonal components of the dipole operator have the property

$$D_{xx} + D_{yy} + D_{zz} \equiv 0\ ,$$

and hence

$$I_{xx}(1,2) = -\tfrac{1}{2} I_{zz}(1,2)\ .$$

The validity of Eq. (26) can again be seen by inspection of Fig. 1 and realizing that under the transformation $z \to -z$, D_{zz} remains invariant.

The proofs of Eqs. (27)–(33) can be obtained using similar symmetry arguments which are fully discussed in Ref. 18.

APPENDIX B: RELATIONS BETWEEN THE INTEGRAL PARAMETERS

It is of interest to consider possible relations between the integral parameters I_{zz}, I_1, and I_2. We shall discuss these relations in terms of two new parameters η and ξ, defined as

$$\xi I_{zz} \equiv \eta I_1 \equiv -I_2\ .$$

It will be shown that when a näive model of the equivalent orbitals is used, η and ξ are simple fractions.

If the equivalent orbitals are approximated by MO-LCAO,

$$\chi_1(x,\ y,\ z) = (\Phi_b \pm \Phi_a)/2N\ ,$$

where N is a normalization constant and

$$\Phi_b = s_b(r) + (x+y+z)\,p_b(r) + (xy+yz+xz)\,d_b(r) + \cdots\ ,$$

where $s_b(r)$, $p_b(r)$, and $d_b(r)$ are radial functions centered on site b. (We consider only σ-type orbitals.) Since the conduction band of silicon is composed primarily of $n=3$ atomic states, we shall ignore f and higher angular momentum states.

We have examined the results of the MO-LCAO approximation in detail for sp^3 hybrids formed from silicon-atom wave functions.[18] These calculations show that the main contribution comes from the atomic orbitals located on the site of interest and contributions involving orbitals on the nearest-neighbor sites are about 1% of the total.

These approximations yield

$$\begin{aligned}
\eta = -I_2/I_1 &= -[\langle s+(-x-y+z)p+(xy-yz-xz)d|\, D_{xy}\,|\, s+(x+y+z)p+(xy+yz+xz)d\rangle] \\
&\quad\times[\langle s+(x+y+z)p+(xy+yz+xz)d|\, D_{xy}\,|\, s+(x+y+z)p+(xy+yz+xz)d\rangle]^{-1} \\
&= (\langle p|\, 3x^2y^2/r^5|\,p\rangle + \langle d|\, 3x^2y^2z^2/r^5|\,d\rangle - \langle s|\, 3x^2y^2/r^5|\,d\rangle) \\
&\quad\times(\langle p|\, 3x^2y^2/r^5|\,p\rangle + \langle d|\, 3x^2y^2z^2/r^5|\,d\rangle + \langle s|\, 3x^2y^2/r^5|\,d\rangle)^{-1} \\
&= (P^2 + \tfrac{1}{7}D^2 - SD)\,(P^2 + \tfrac{1}{7}D^2 + SD)^{-1}\ ,
\end{aligned}$$

where

$$P^2 = \int_0^R p^2 r\,dr, \quad D^2 = \int_0^R d^2 r^3\,dr\ ,$$

and

$$SD = \int_0^R s\,dr\,dr\ .$$

Similarly, we obtain

$$\xi = -I_2/I_{zz} = (P^2 + \tfrac{1}{7}D^2 - SD)(\tfrac{4}{7}P^2 - \tfrac{4}{21}D^2)^{-1}\ .$$

The approximation of sp^3 hybrids is obtained by setting $d=0$. In this case, we have $\xi=\frac{3}{4}$ and $\eta=1$. The fact that the sp^3-hybrids approach is a poor approximation is illustrated by noting that this predicts $B_{xy}(0, 0, 4)$ to be zero when, in fact, it is large (see Table III). [It was noted by Feher[4] that d character was needed to explain $B_{xy}(0, 0, 4)$.]

*Work supported in part by Army Research Office and National Science Foundation.

†Present address: Department of Physics, University of Missouri-Rolla, Rolla, Mo.

[1]J. M. Luttinger and W. Kohn, Phys. Rev. 97, 869 (1955).

[2]W. Kohn and J. M. Luttinger, Phys. Rev. 98, 915 (1955).

[3]W. Kohn, in *Solid State Physics*, edited by F. Seitz and D. Turnbull (Academic, New York, 1957), Vol. 5.

[4]G. Feher, Phys. Rev. 114, 1219 (1959).

[5]E. B. Hale and R. L. Mieher, Phys. Rev. 184, 739 (1969).

[6]E. B. Hale and R. L. Mieher, Phys. Rev. 184, 751 (1969).

[7]A preliminary account of this work has appeared in E. B. Hale and R. L. Mieher, Phys. Letters 29A, 350 (1969).

[8]G. G. Hall, Phil. Mag. 43, 338 (1952); Proc. Phys. Soc. (London) A66, 1162 (1953).

[9]G. G. Hall, Phys. Rev. 90, 317 (1953); Phil. Mag. 3, 429 (1958).

[10]The values used for these constants in the numerical calculations were $a_l=14.2$ Å, $a_t=25.0$ Å, $a^*=21.0$ Å, $n(\mathrm{As})=0.736$, $n(\mathrm{P})=0.800$, and $n(\mathrm{Sb})=0.826$. Various calculations using the envelope function in Eq. (2) have been discussed in Ref. 6.

[11]J. C. Slater and G. F. Koster, Phys. Rev. 94, 1498 (1954).

[12]F. Herman, Phys. Rev. 88, 1210 (1952).

[13]L. B. Redei, Proc. Roy. Soc. (London) A270, 373 (1962); A270, 383 (1962); D. Stocker, *ibid.* A270, 397 (1962); J. A. R. Coope, Ph. D. thesis, Oxford University, 1956 (unpublished), cited in above references; and N. V. Cohan, D. Pugh, and R. H. Tredgold, Proc. Phys. Soc. (London) 82, 65 (1963).

[14]In Refs. 8 and 9, Hall used a fitting procedure to obtain expressions for the band energies along the symmetry directions. This procedure has also been used by D. L. Spears, M. A. thesis, Dartmouth College, 1964 (unpublished).

[15]W. A. Harrison, *Pseudopotentials in the Theory of Metals* (Benjamin, New York, 1966), and references cited therein.

[16]G. Dresselhaus and M. S. Dresselhaus, Phys. Rev. 160, 649 (1967).

[17]P. W. Anderson, Phys. Rev. Letters 21, 13 (1968).

[18]These calculations are discussed in detail in E. B. Hale, Ph. D. thesis, Purdue University, 1968 (unpublished).

[19]J. L. Ivey and R. L. Mieher (unpublished).

[20]The available data on the location of k_0 are discussed in detail by E. B. Hale and T. G. Castner, Jr., Phys. Rev. B 1, 4763 (1970).

[21]One check on our formulation of the wave function in terms of equivalent orbitals is that we obtain the same expression for the contact interaction that is discussed in Refs. 4 and 6.

[22]A recent improvement [R. A. Faulkner, Phys. Rev. 184, 713 (1969)] in the effective-mass approach has yielded accurate values for the energies of the excited states of the shallow donors. However, the problems of the ground-state wave functions and energies are related to the "chemical-shift" phenomenon and are not related to the approximations in the solution of the effective-mass Hamiltonian.

PHYSICAL REVIEW B VOLUME 3, NUMBER 6 15 MARCH 1971

Longitudinal Optical Phonons in Thin Films of CdS, CdSe, and Their Mixtures

G. Lubberts*
Department of Electrical Engineering, University of Rochester, Rochester, New York 14627
(Received 28 September 1970)

LO phonon energies have been determined by means of electron tunneling in Sn-SnO-semiconductor-Sn junctions. For mixtures of CdS and CdSe, we find two distinct structures in the tunneling data which occur at lower energies than the LO phonons for pure CdS and CdSe. These results agree with infrared spectroscopic data on bulk crystals. This agreement provides strong evidence that only short-range forces are important in determining the optical-phonon spectra.

In recent experiments, Giaever and Zeller[1-3] as well as MacVicar *et al.*,[4] have demonstrated that it is possible for electrons to tunnel through thin layers of semiconducting materials which are sandwiched between two metal films. By examining the current-voltage (I-V) curve of such tunneling junctions, Giaever and Zeller[2,3] found a resistance decrease in such devices at applied voltages corresponding to the longitudinal optical (LO) phonon energy of the semiconductor material. Such resistance changes are usually observable when first- or second-derivative measurements are made of the I-V curve. The decrease in resistance can be explained by considering the interaction of the tun-